

# Adsorption of Reactive Dye Using Entrapped nZVI

P. Gomathi Priya, M. E. Thenmozhi

**Abstract**—Iron nanoparticles were used to cleanup effluents. This paper involves synthesis of iron nanoparticles chemically by sodium borohydride reduction of ammonium ferrous sulfate solution (FAS). Iron oxide nanoparticles have lesser efficiency of adsorption than Zero Valent Iron nanoparticles (nZVI). Glucosamine acts as a stabilizing agent and chelating agent to prevent Iron nanoparticles from oxidation. nZVI particles were characterized using Scanning Electron Microscopy (SEM). Thus, the synthesized nZVI was subjected to entrapment in biopolymer, viz. barium (Ba)-alginate beads. The beads were characterized using SEM. Batch dye degradation studies were conducted using Reactive black Water soluble Nontoxic Natural substances (WNN) dye which is one of the most hazardous dyes used in textile industries. Effect of contact time, effect of pH, initial dye concentration, adsorbent dosage, isotherm and kinetic studies were carried out.

**Keywords**—A Ammonium ferrous sulfate solution, barium (Ba)-alginate beads, reactive black WNN dye, zero valent iron nanoparticles.

## I. INTRODUCTION

WASTEWATER treatment has become a challenging task in order to make it usable. Dying industries let out effluents into water bodies that contain hazardous carcinogenic dyes containing azo groups. This threatens the life of aquatic habitat and habitation around the water bodies. It also affects economic up growth and ancient customs of locales. The most commonly used methods for color removal are biological and chemical precipitation [1]. Although these processes are efficient and cost-effective considerably, solute concentrations are relatively high [2]. Even though many methods were explored to address this environmental and economic concern, there are advantages and disadvantages in each and every method used for dye removal from wastewaters [3]. Many physicochemical methods have been tested, but adsorption is considered to be superior to other techniques. Reactive black Water soluble WNN dye has dual azo group that is carcinogenic when mixed in drinking water. Iron nanoparticle technology has high surface area that enhances its surface reactivity towards effluent treatment [4]. Iron nanoparticles oxidize as soon as its formation and it retards adsorption process. Over the last few years, various synthetic methods have been developed to produce iron nanoparticles [2]. This paper majorly involves the synthesis of nZVI from Fe (II) (ferric) or Fe (III) (ferrous) aqueous

solution by reducing it using sodium borohydride [8]. The nZVI produced by chemical synthesis is unstable due to its highly oxidative character [5]. In order to stabilize nZVI particles, several stabilizing agents are added to the aqueous ferrous solution. The stabilizing agent could be used as chelating agents, dispersants in ferrous aqueous solution. Stabilization agents protect the iron nano particles from oxidation [6]. Stabilization agents involving chelating agents cover the nanoparticle's surface thereby preventing oxidation. Due to loss of particles during adsorbent recovery, nZVI was subjected to immobilization using bio-polymer of alginate. Stabilized nZVIs were subjected to immobilization by means of bio-polymer of barium alginate [7].

## II. MATERIALS AND EXPERIMENTAL METHODS

### A. Materials

The chemical reagents used in the preparation of nZVI were: Ammonium ferrous sulfate hexahydrate was purchased from Merck India. Sodium borohydride, Glucosamine Hydrochloride (98%) and 99.99% ethanol were purchased from Aldrich Chemicals. Reactive black WNN dye was purchased in Chennai chemicals. In general, there were two main parts in this research; where the first part was synthesis of nZVI and the second part was immobilizing it using bio-polymer of barium alginate. After immobilization, the beads entrapped nZVIs were subjected to dye solution and carried out for adsorption studies.

### B. Synthesis of nZVI

150 ml of 0.05 M FAS, 100 ml of 0.15 M of glucosamine and 100 ml of 0.05 M sodium borohydride were prepared using distilled water. The reaction was carried out in a three neck round bottomed flask where FAS solution was added along with stabilizing agent. Sodium borohydride was added drop wise to the solution. Black color nZVI particles were observed in the three-neck round bottomed flask fitted with a mechanical stirrer operated at 230 rpm. nZVI particles were centrifuged at 2000 rpm for 20 minutes. The nZVI particles were washed thrice using 99.99% ethanol and dried in vacuum oven at 75 °C. The dried particles were scrubbed and powdered using mortar and pestle.

### C. Immobilization of nZVI

After zerovalent iron nanoparticles synthesis, it was subjected to immobilization procedure. A solution containing nZVI (2 wt. %) and sodium alginate (2 wt. %) was prepared with distilled water and stirred for 30 minutes at 85 °C in an oil bath. Another solution of Barium chloride (12 wt. %) was prepared with distilled water and kept in stirring. The solution of nZVI particles and sodium alginate was extruded as small drops by means of a syringe into the Stirred solution of barium

P. Gomathi Priya (Associate Professor) is with the Department of Chemical Engineering, Alagappa College of Technology, Anna University, Chennai -600025, India (Corresponding author; phone: 044 22359138, pgpriyachem@gmail.com).

M. E. Thenmozhi (PG student) is with the Department of Chemical Engineering, Alagappa College of Technology, Anna University, Chennai-600025.

chloride (12 wt.%). Formation of spherical gel beads of 4-5 mm was observed. The gel beads were retained in the barium chloride solution for 12 hours for hardening. The gel beads were retrieved and washed with distilled water and used for dye adsorption studies.

#### D. Dye Removal by Adsorption

Reactive black WNN dye was dissolved in distilled water and stock solution of 100 ppm was prepared. The stock solution was diluted to concentrations varying from 10-50 ppm. 5 ml of 10% hydrogen peroxide was added to each concentration to enhance adsorption [8]. Adsorbent dosages of 0.1 g, 0.3 g, 0.6 g, 1.0 g of nZVI were entrapped in barium alginate beads and studied. Batch studies were conducted in conical flasks which were kept in shaker at 100 rpm. Samples were taken at predetermined time intervals. The final concentrations of Reactive black WNN were analyzed using a UV-Vis spectrophotometer.

### III. RESULTS AND DISCUSSION

#### A. SEM Results of nZVI and Barium Alginate Beads Entrapped nZVI

The iron nanoparticles synthesized using glucosamine as stabilizing agent show fairly stable characteristics. The chelating agent concentration is thrice the molarity of Ammonium ferrous sulphate (FAS). nZVIs chemically were characterized using SEM. The external morphology of SEM image (Fig. 1) features that the iron nanoparticles were spherical in shape of various diameters in nanometer. The image was taken at a resolution of 54.8 kx (500 nm) magnification. SEM image was also taken at 11.3 kx magnification. The particles were magnified at a scale of 2  $\mu$ m. Fig. 2 shows that the particles were clusters of spherical nZVI particles of various diameters [9]. The iron nanoparticles are loosely bound in powder form. Barium alginate beads entrapped nZVI was characterized using SEM. SEM image at 4.62 kx (5  $\mu$ m) magnification of the Ba-Alginate bead was porous and flaky as shown in Fig. 3. The size of each pore would be less than 0.5  $\mu$ m. The strength of alginate beads depends on the concentration of barium chloride and sodium alginate solutions. As soon as the bead formation in the solution there would be high moisture content that can be gradually decreased by drying in atmospheric air. Fig. 4 shows that 100 times magnified sectional view of barium alginate bead that shows that the surface of the bead was porous, and the internal structure was bit flaky and porous. The image was taken at a scale of 200  $\mu$ m. The porous structure would enhance the permeability of small molecules and allows solutes to diffuse into the beads and come in contact with the entrapped material.

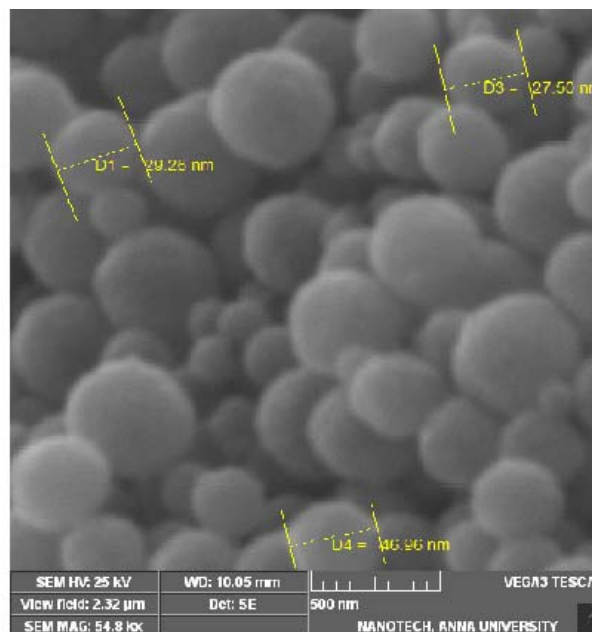


Fig. 1 SEM image of nZVI at 500 nm

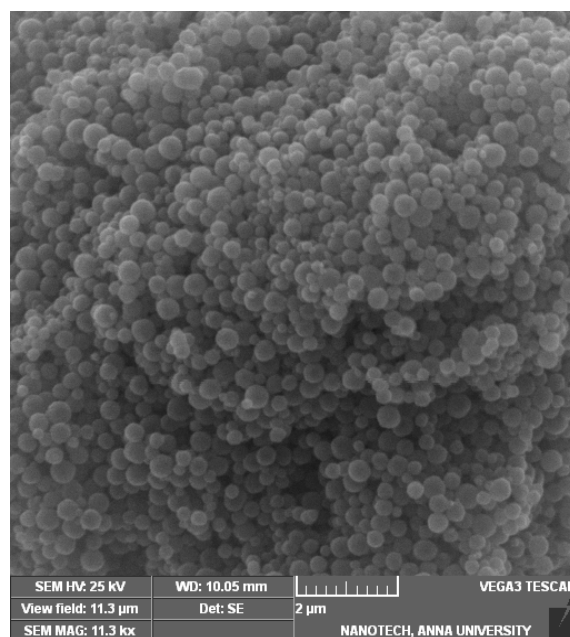


Fig. 2 SEM image of nZVI at 2  $\mu$ m

#### B. Batch Studies of Dye Removal

Effect of contact time, effect of pH, effect of initial dye concentration and effect of adsorbent dosage were studied. The percentage color removal was found to be 98.88 % at 10 ppm of adsorbent dosage. The equilibrium time was achieved at 240 minutes as shown in Fig. 5. The zero-point charge of iron nanoparticles was at pH 8 [10] (Fig. 6). Effect of zero-point charge was studied to determine the pH where the nZVI particles attain zero charge on its surface. This study was conducted in NaCl solution to which 0.5 M HCl and 0.5 M NaOH were added to adjust the pH. 0.1 g of nZVI entrapped barium alginate beads were added to 50 ml solution of various

pH (pH 2- 14) and kept in shaker for 48 hours [10]. The percentage removal was found to be higher at alkaline pH (10, 12 and 14) [11] (Figs. 7-9). Hydrogen peroxide when added evolves H<sup>+</sup> ion that enhances adsorption due its competence with dye to the negative adsorptive sites of adsorbent resulting higher removal at alkaline range [12]. At pH 12 and 14, the beads entrapped nZVI started breaking down rapidly; so the pH was optimized at 10 where beads were not affected.

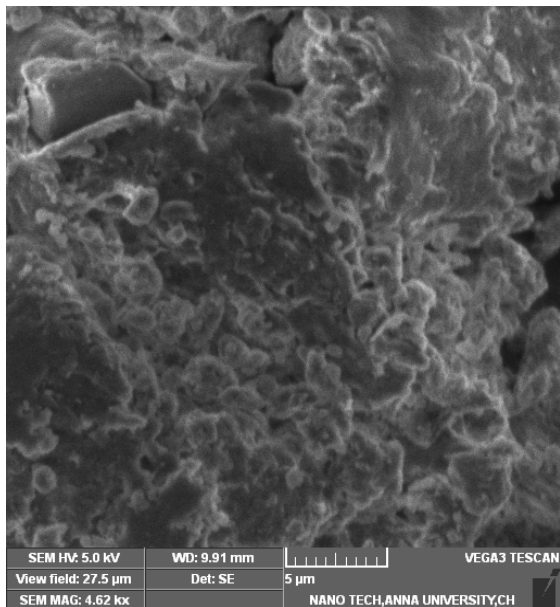


Fig. 3 SEM image of barium alginate entrapped nZVI at 5 μm

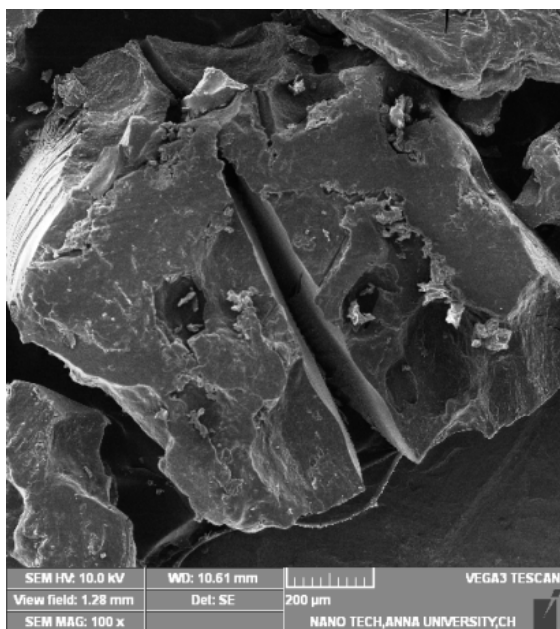


Fig. 4 SEM image of barium alginate entrapped nZVI at 200 μm

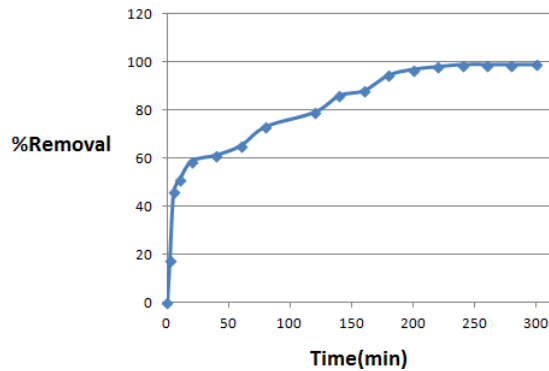


Fig. 5 Effect of contact time

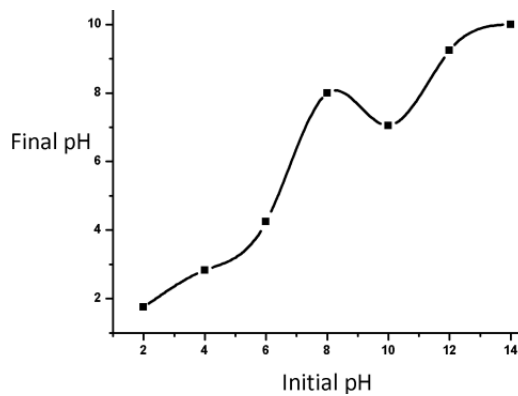


Fig. 6 Effect of zero-point charge

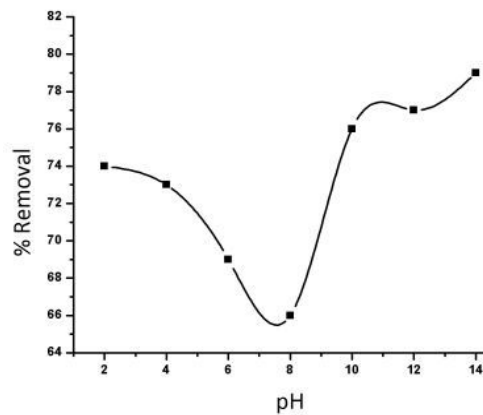


Fig. 7 Effect of pH

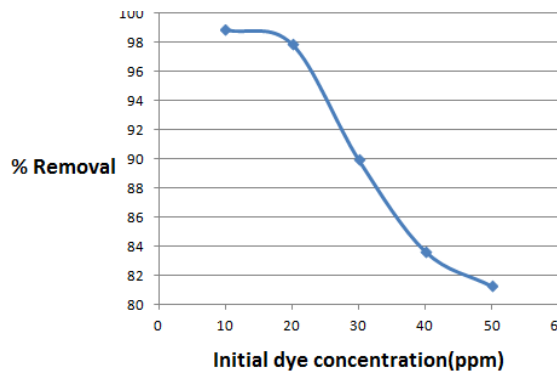


Fig. 8 Effect of initial dye concentration

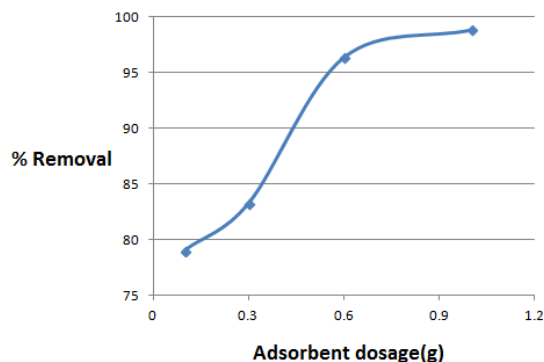


Fig. 9 Effect of adsorbent dosage

### C. Adsorption Isotherms

The monolayer Langmuir and the empirical Freundlich isotherms that can be applied to explain the equilibrium adsorption characteristics are known as the most commonly used models. The linear forms of these equations are mentioned below as (1) (Langmuir) and (2) (Freundlich).

$$\frac{1}{q_e} = \frac{1}{q_m} + \frac{1}{K_1 q_m C_e} \quad (1)$$

$$\log q_e = \log K_f + \frac{1}{n} \log C_e \quad (2)$$

where  $q_m$  ( $\text{mg g}^{-1}$ ) is the maximum adsorption capacity,  $q_e$  ( $\text{mg g}^{-1}$ ) is the amount of adsorbed dye,  $C_e$  ( $\text{mg L}^{-1}$ ) is the equilibrium dye concentration,  $K_f$  and  $n$  are the Freundlich constants, and  $K_1$  ( $\text{L mg}^{-1}$ ) is the Langmuir constant [13]. The experimental data were fitted both in Langmuir and Freundlich isotherms (Figs. 10, 11 and Table I).

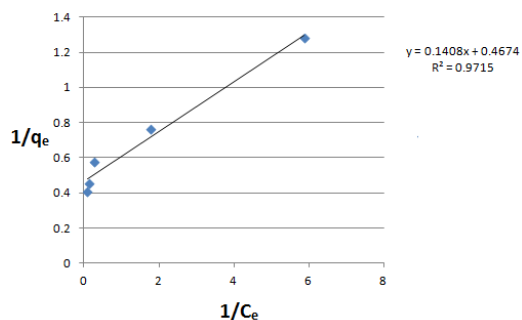


Fig. 10 Langmuir adsorption isotherm plot

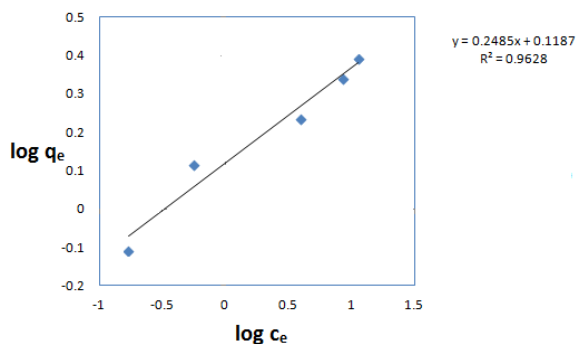


Fig. 11 Freundlich adsorption isotherm plot

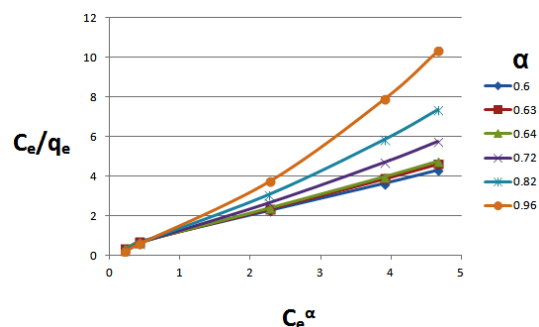


Fig. 12 Redlich-Peterson isotherm plot

TABLE I  
ISOTHERM AND KINETIC MODEL CONSTANTS

Isotherm	Parameters	Constants
Langmuir	Adsorption capacity $q_m$	2.137 (mg/g)
	Langmuir constant $K_1$	3.32 (L/mg)
	Regression Coeff $R^2$	0.9715
Freundlich	Sorption Capacity $K_f$	1.314 (L/mg)
	Sorption intensity $n$	4.02
	Regression Coeff $R^2$	0.9628
Redlich perterson	R-P constant $b_{RP}$	4.443
	$q_{mon}$	1.03
	$\alpha$	0.64
	Regression Coeff $R^2$	0.9995
Elovich	Initial adsorption rate $\alpha$	0.22 $\text{mg g}^{-1} \text{min}^{-1}$
	adsorption constant $\beta$	2.308g/mg
	Regression Coeff $R^2$	0.9875

### D. Redlich-Peterson (R-P) Isotherm Equation

The R-P isotherm equation amends inaccuracies of two parameter Langmuir and Freundlich isotherm equations in some adsorption systems [14].

$$\frac{C_e}{q_e} = \frac{1}{b_{RP} q'_{mon}} + \frac{1}{q'_{mon}} C_e^\alpha \quad (3)$$

Equation (3) is the exponential linear form obtained by plotting  $C_e/q_e$  vs.  $C_e^\alpha$ . By trial and error, this study adopted  $\alpha$  value for the optimum line. In the specific range,  $\alpha$  value is limited and it is easy to obtain the correct value [13]. Fig. 12 and Table I show the R-P plot for different  $\alpha$  values. The regression-coefficient value is at higher at  $\alpha=0.64$  ( $R^2=0.9995$ ). By trial and error method, regression-coefficient was found to decrease when  $\alpha$  value reduced below 0.6 as well as when increased beyond 0.7. R-P plot is more accurate than Langmuir and Freundlich isothermal plots [13], [15].

### E. Kinetic Studies

To evaluate the mechanism of adsorption process using mass transfer and chemical reaction, the rate data were examined to find a suitable kinetic model.

### F. Simple First Order Model

$$\log C_t = \frac{K_1}{2.303} t + \log C_0 \quad (4)$$

where  $C_t$  and  $C_0$  are the concentration of dye at time  $t$  and initially ( $\text{mg L}^{-1}$ ), respectively.  $K_1$  is the first order rate

constant ( $\text{min}^{-1}$ ) shown in Fig. 13.

*G. Pseudo- First Order Model*

$$\log (q_e - q_t) = \log q_e - K_1 t \quad (5)$$

where  $q_e$  and  $q_t$  are amounts of dye adsorbed at equilibrium and at time  $t$  ( $\text{mg g}^{-1}$ ), respectively, and  $K_1$  is the equilibrium rate constant of pseudo first-order adsorption, ( $\text{min}^{-1}$ ) (Fig. 14).

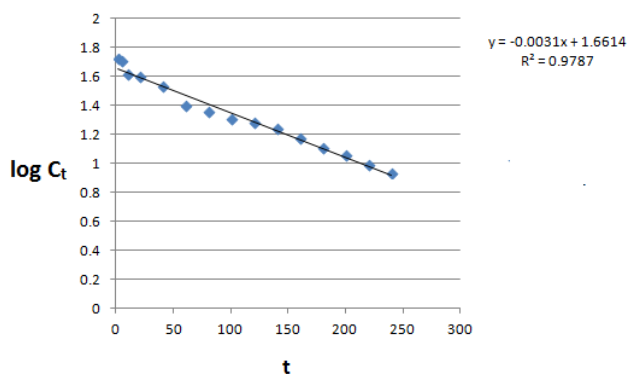


Fig. 13 Simple-first order model

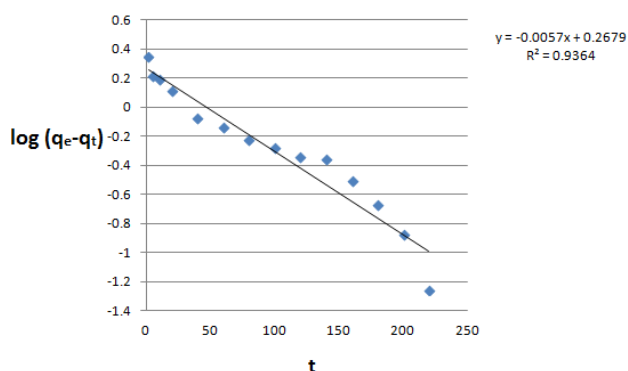


Fig. 14 Pseudo-first order model

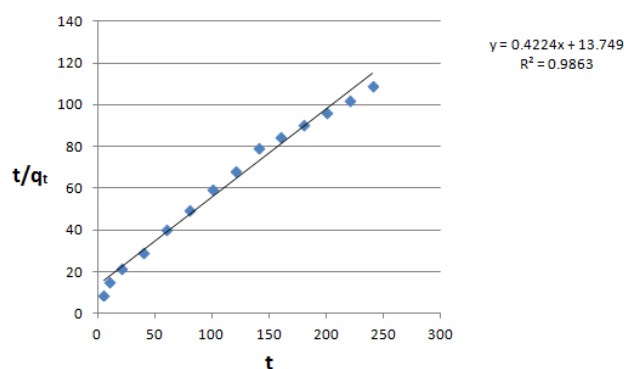


Fig. 15 Pseudo-second order model

*H. Pseudo-Second Order Model*

$$\frac{t}{q} = \frac{1}{K_2 q_e^2} + \frac{t}{q} \quad (6)$$

where  $K_2$  is the equilibrium rate constant of pseudo second-

order adsorption ( $\text{g mg}^{-1} \text{min}^{-1}$ ). The slopes and intercepts of plots  $t/q$  versus  $t$  were used to calculate the pseudo second-order rate constants  $K_2$  and  $q_e$  (Fig. 15).

*I. Elovich Model*

$$q_t = \frac{1}{\beta} \ln (\alpha \beta) + \frac{1}{\beta} \ln (t) \quad (7)$$

where  $\alpha$  is the initial adsorption rate ( $\text{mg g}^{-1} \text{min}^{-1}$ ), and  $\beta$  is the adsorption constant ( $\text{g mg}^{-1}$ ) which is shown in Fig. 16 and Table I.

*J. Intra -Particle Diffusion Model*

$$q_t = K_t t^{1/2} + c \quad (8)$$

where  $C$  is the intercept and  $K_t$  is the intra-particle diffusion rate constant ( $\text{mg g}^{-1} \text{min}^{-1}$ ), which can be evaluated from the slope of the linear plot of  $q_t$  versus  $t^{1/2}$  [13] which is confirmed in Fig 17.

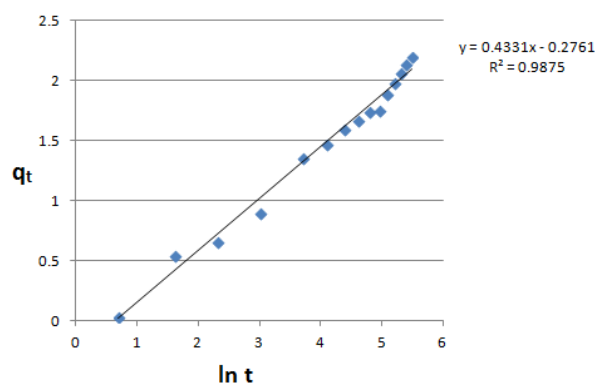


Fig. 16 Elovich model

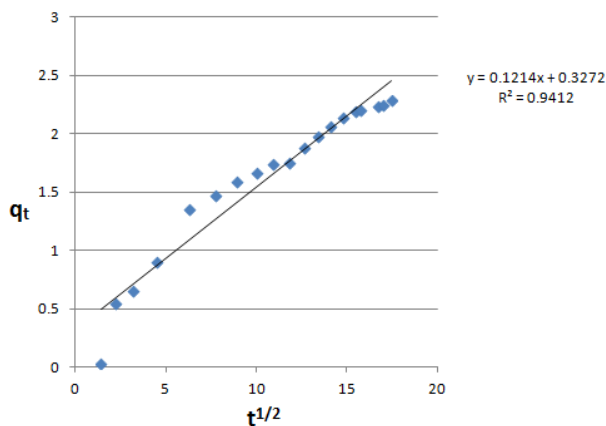


Fig. 17 Intra-particle diffusion model

*K. Desorption and Recycling*

The nZVI entrapped beads after adsorption treatment was kept in dilute HCl solution at 0.01 M and then washed in 99.99% ethanol. The desorbed nZVI beads were again subjected to adsorption in 10 ppm dye solution at pH 10 (Fig. 18).

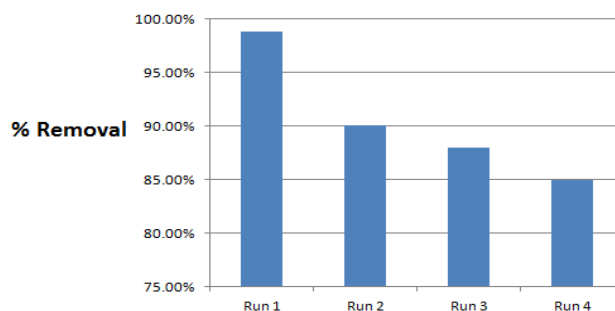


Fig. 18 Recycle chart

#### IV. CONCLUSION

Adsorption kinetic and isotherm parameters of Reactive black WNN on nZVI entrapped barium alginate beads were studied in a batch system. Percentage color removal was dependent on the contact time, pH of the solution, adsorbent dosage and initial dye concentration. The maximum amount of reactive black WNN removal from synthetic effluent for nZVI entrapped barium alginate beads was found to be at the contact time of 240 min. Maximum color removal was achieved at 98.88% at 10 ppm of nZVI adsorbent dosage. The experimental data obtained mostly fitted in Redlich-Peterson isotherm equation where the regression-coefficient was 0.9995. The kinetics of adsorbents was experimentally studied and examined using the simple first order, pseudo first-order, pseudo second-order and Elovich kinetic models. According to the values of the correlation coefficient ( $R^2$ ) obtained for all tested models, Elovich model was stated to the best correlate the rate kinetic data of nZVI entrapped barium alginate beads ( $R^2=0.9875$ ). Desorption and recycling of barium alginate beads was done successfully.

#### REFERENCES

- [1] Malik A and Taneja U, "Utilizing fly ash for color removal of dye effluents" *Am Dyestuff Rep*, vol 83, pp. 20–27, 1994.
- [2] T. Mahmood, M. T. Saddique, A. Naeem, P. Westerhoff, S. Mustafa and A. Alum, "Utilization of Pine Nut Shell derived carbon as an efficient alternate for the sequestration of phthalates from aqueous system," *Ind. Eng. Chem. Res*, vol 50, pp. 100–117, 2011.
- [3] Utsumi H, Han YH and Ichikawa K, "A kinetic study of 3-chlorophenol enhanced hydroxyl radical generation during ozonation," *Water Res*, vol 37, pp. 4924–4928, 2003.
- [4] V. Vadivelan and Kumar KV, "Equilibrium, kinetics, mechanism, and process design for the sorption of methylene blue onto rice husk," *J Colloid Interface Sci*, vol 286, pp. 90–100, 2005.
- [5] H. Paul Wang, Jiasheng Cao, Wei-xian Zhang, Xiao-qin Li and Yuan-Pang Sun, "Characterization of zero-valent iron nanoparticles," *Advances in Colloid and Interface Science*, vol.120, pp.47–56, 2006.
- [6] Badal Kumar Mandal, Koppala Siva Kumar, Murad Basha Allabaksh, Mohan Kumar Kesarla and Pamanji Sreedhara Reddy, "Preparation of Stable Zero Valent Iron Nanoparticles using Different Chelating Agents" *Journal of Chemical and Pharmaceutical Research*, vol 2, no 5, pp. 67–74, 2010.
- [7] P. S. Harikumar and Litty Joseph, "Kinetic and thermodynamics studies of As (III) adsorption onto iron nanoparticles entrapped Ca-alginate beads," *International Journal of Plant, Animal and Environmental Sciences*, vol 2, pp. 159–166, 2012.
- [8] Dionysios D. Dionysiou, Makram T. Suidana, Evangelia Bekoua, Isabelle Baudin and Jean-Michel La'ne b, "Effect of ionic strength and hydrogen peroxide on the photocatalytic degradation of 4-chlorobenzoic acid in water," *Applied Catalysis B: Environmental*, vol 26, pp.153–171, 2000.

- [9] Cissoko Naman, Xinhua Xu, Qian Wang, Huijing Qian, Yueping Yang and Zhen Zhang, "Reduction of hexavalent chromium by carboxymethyl cellulose-stabilized zero-valent iron nanoparticles" *Journal of Contaminant Hydrology*, vol 114, pp. 35–42, 2010.
- [10] Marek Kosmulski, "pH-dependent surface charging and points of zero charge. IV. Update and new approach," *Journal of Colloid and Interface Science*, vol 337, pp. 439–448, 2009.
- [11] Aamir D. Abid, Masakazu Kanematsu, Thomas M. Young, and Ian M. Kennedy, "Arsenic removal from water using flame-synthesized iron oxide nanoparticles with variable oxidation states," *Aerosol Sci Technol*, vol 47, no 2, pp. 169–176, 2013.
- [12] Saideh Adami and Ali Fakhri, "Adsorption of 4-Chloro-2-Nitrophenol by Zero Valent Iron Nanoparticles and Pd-Doped Zero Valent Iron Nanoparticles Surfaces: Isotherm, Kinetic and Mechanism Modeling," vol 10, pp.2–16, 2013.
- [13] S. M. Yakout and E. Elsharif, "Batch kinetics, isotherm and thermodynamic studies of adsorption of strontium from aqueous solutions onto low cost rice-straw based carbons," *Carbon – Sci. Tech*, vol 1, pp. 144 – 153, 2010.
- [14] Feng-Chin Wu, Bing-Lan Liu, Keng-Tung Wu and Ru-Ling Tseng, "A new linear form analysis of Redlich–Peterson isotherm equation for the adsorptions of dyes," *Chemical Engineering Journal*, vol 162, pp.21–27, 2010.
- [15] Lidija Ćurković, Alenka Rastovčan-Mioč<sup>1</sup>, Marijana Majić and Josip Župan, "Application of different isotherm models on lead ions sorption onto electric furnace slag," *The holistic approach to environment*, vol 1, pp.13–18, 2011.